Polymer xxx (2013) 1–9

Contents lists available at ScienceDirect

Polymer

journal homepage: www.elsevier.com/locate/polymer

Effect of molecular parameters on thermomechanical behavior of side-on nematic liquid crystal elastomers

Renbo Wei [a], Lingyun Zhou [a], Yaning He [a], Xiaogong Wang [a,*], Patrick Keller [b,**]

[a] Department of Chemical Engineering, Key Laboratory of Advanced Materials (MOE), Tsinghua University, Beijing 100084, People's Republic of China
[b] Institut Curie, Centre de Recherche, CNRS UMR 168, Université Pierre et Marie Curie, 26 rue d'Ulm, 75248 Paris Cedex 05, France

ARTICLE INFO

Article history:
Received 12 March 2013
Received in revised form
28 June 2013
Accepted 21 July 2013
Available online xxx

Keywords:
Liquid crystal elastomers
Thermomechanical behavior
Molecular parameters

ABSTRACT

We investigated the structure–property relationship of liquid crystal elastomers (LCEs) obtained from a series of nematic side-on monomers. A new synthetic strategy was developed to obtain the acrylate monomers (*n*-ADBB), which gave us the opportunity to easily modify the spacer lengths of the monomers. Through magnetic field alignment, well-defined LCE micropillars were fabricated from the monomers by a method combining soft lithography and photopolymerization/photocrosslinking of the monomers and a crosslinker. The influence of structural parameters on the thermomechanical deformation of the microstructures was studied through microscopic observations. The study quantitatively revealed the correlation of thermomechanical behavior of the microstructured LCEs with the crosslinking density and length of the flexible spacer linking the mesogenic core to the backbone. With a proper control of the structural parameters, optimized performances such as large reversible contraction, good elasticity and mechanical robustness were demonstrated for this type of LCEs.

1. Introduction

Liquid crystalline elastomers (LCEs) have been intensively investigated in recent years owing to their fascinating properties and potential applications [1–10]. Combining anisotropic orientation of liquid crystals (LCs) with the rubbery elasticity of polymer networks, the materials are endowed with specific properties, such as stimuli-induced reversible deformation and anisotropic shape changes. Depending on the LC phases exhibited by the systems, LCEs are divided into nematic LCE [11], smectic LCE [8], and others. The nematic LCE with uniform spatial orientation is the simplest and most widely studied type among them. In a nematic LCE, the average macromolecular shape is coupled with the orientational nematic order [1,12]. The polymer chains elongate when their mesogens orient in the nematic phase, while in the isotropic phase, they recover a random coil conformation, driven by entropy [12]. At the nematic–isotropic phase transition, a change in the average molecular shape from elongated to coiled conformations will be triggered and translated at a macroscopical level to induce a shape deformation of the elastomer sample. Making use of the sensitivity of mesophases to various physical stimuli, LCEs with thermo-responsive [13,14], photo-responsive [15,16], and electro-responsive [17–19] functions have been developed. In recent years, their applications as artificial muscles [20], micropumps and microvalves for microfluidic devices [21–23], and opto-mechanical shutters [24], have been actively explored.

Understanding structure–property relationship of the LCEs is extremely important for optimizing properties and achieving real applications. Different LCEs with the mesogenic units in the main-chain and side-chains have been synthesized and investigated [2,3,8,11,25–27]. For the LCEs with side-chain architecture, both "end-on" and "side-on" LCEs, depending on whether the mesogenic groups are attached terminally or laterally to the polymer backbone via a flexible spacer, have been developed and intensively investigated [2,3,8,11,25]. For liquid crystal polymers (LCPs) and LCEs, the end-on structure usually tends to form a smectic phase, especially for those with longer spacers [28]. On the other hand, the nematic phase is favored in "side-on" LCPs and LCEs, in which the mesogens are laterally attached to the polymer backbone [29–32]. In addition to the mesogen-attaching mode, the mesomorphic properties of LCPs and LCEs are also closely related to mesogenic units [33], linking groups [34].

There are several critically important issues need to be addressed in order to further understand the structure–property

* Corresponding author. Tel.: +86 10 62784561; fax: +86 10 62770304.
** Corresponding author. Tel.: +33 (0)1 56246762; fax: +33 (0)1 40510636.
E-mail addresses: wxg-dce@mail.tsinghua.edu.cn (X. Wang), patrick.keller@curie.fr (P. Keller).

0032-3861/$ – see front matter © 2013 Elsevier Ltd. All rights reserved.
http://dx.doi.org/10.1016/j.polymer.2013.07.057

relationship. The spacer length and crosslinking density are two key control factors that need to be studied. The spacer length determines the coupling strength between the side-chain mesogenic units and the backbone, which plays an important role to influence the molecular shape change during the phase transition. Crosslinking density controls the topological restrain between the polymeric chains and affects the mechanical properties related to the chain conformation [35]. In order to explore the structure–property relationship, nematic LCEs with uniaxial alignment and mono-domain (named 'liquid single crystal elastomer' by Finkelmann [36]) are required. The 'liquid single crystal elastomer' samples have been obtained by methods such as stretching pre-crosslinked films [2,4,8], drawing fibers from a polymer melt [9], crosslinking in liquid crystalline cells [3,16], aligning with electric or magnetic fields [13,14], and others [6,37–40]. Among them, obtaining a regular array of pillar-like microstructures by soft-lithography and magnetic field alignment is an appealing new approach [13,14]. Although many efforts have been devoted to the LCE study, to our knowledge, a systematic study on the effects of the spacer length and crosslinking density by using the well-defined microstructures has not been reported in the literature yet.

In this study, influences of crosslinking density and spacer length on the properties of the side-on LCEs were investigated by using pillar-like microstructures obtained by the method combining soft-lithography and magnetic field alignment. In order to keep the LCEs all in the nematic phase, the side-on nematic monomers with different spacer length were selected. An improved strategy was developed to synthesize side-on LC acrylate monomers with the different spacer lengths. Monomers with different spacer lengths, which contained 2, 3, 4, 5 and 6 methylenes (*n*-ADBB, *n* representing the numbers of the methylenes), were synthesized and characterized by ^{1}H NMR, ^{13}C NMR, FT-IR, POM and DSC. The monomers were first mixed with the crosslinking agent in different ratios and a suitable amount of the photoinitiator. Then, LCE pillars were prepared with the mixture by the soft-lithographic technique. The effects of the crosslinking density and spacer length were studied by microscopically characterizing thermomechanical properties of the LCE micropillars, which were separated from the substrates. The correlation of thermomechanical behavior of the micro-structured LCEs with the crosslinking density and length of the flexible spacer was quantitatively revealed by the study.

2. Experimental section

2.1. Materials

2,5-Dihydroxybenzoic acid (99%) and 4-n-butyloxybenzoic acid (98%) were purchased from Alfa Aesar and used as received. Crosslinking agent, 1,6-hexanediol diacrylate (98%) was purchased from Adamas-beta and used as received. Photoinitiator, 2-benzyl-2-(dimethylamino)-4′-morpholinobutyrophenone (97%), was purchased from Sigma Aldrich and used as received. Tetrahydrofuran (THF) was purified by distillation with sodium and benzophenone. Deionized water (resistivity $>$ 18 MΩ cm) was obtained from a Milli-Q water purification system. Azo-bis-isobutryonitrile (AIBN) was recrystallized from anhydrous methanol before use. All other reagents were commercially available products and used as received without further purification.

2.2. Characterization

^{1}H and ^{13}C NMR spectra were obtained on a JEOL JNM-ECA300 or JEOL JNM-ECA600 NMR spectrometer with tetramethylsilane (TMS) as the internal standard at ambient temperature in d_6-DMSO or $CDCl_3$. FT-IR spectra were collected on a Nicolet 560-IR spectrometer: the samples were mixed with KBr powder and then pressed into thin transparent disks. The molecular weights and molecular weight distributions were measured using a gel permeation chromatographic (GPC) instrument equipped with a PLgel 5 μm mixed-D column and a refractive index (RI) detector (Wyatt Optilab rEX). The measurements were carried out at 35 °C and the molecular weights were calibrated with polystyrene standards. THF was used as the eluant and the flow rate was 1.0 mL/min. Thermal analyses of the compounds were carried out using TA Instruments DSC Q2000 system with a heating rate of 10 °C/min in a nitrogen atmosphere. Polarizing optical microscopic (POM) observations were conducted on a Nikon LV 1000 POL microscope equipped with a CCD camera and a hot stage. The SEM measurements were performed on a field emission microscope (Hitachi S-4500) with the accelerating voltage of 15 kV. The samples prepared for SEM studies were observed after sputter coating treatment with Au.

2.3. 2″-Acryloyloxyethyl 2,5-di(4′-butyloxybenzoyloxy)benzoate (2-ADBB)

The monomer was synthesized through three-step reactions as shown in Scheme 1. 2′-Bromo-ethyl 2,5-dihydroxybenzoate (A_2) was first obtained from the nucleophilic substitution reaction between 2,5-dihydroxybenzoic acid and 1,2-dibromoethane. Then, 2′-acryloyloxyethyl 2,5-dihydroxybenzoate (B_2) was obtained by reaction between A_2 and acrylic acid. The synthetic details and analytic results of the intermediates are given in the Supporting information. In the final step, a solution of B_2 (2.5 g, 10 mmol), 4-n-butyloxybenzoic acid (4.1 g, 21 mmol), N,N-dicyclohexylcarbodiimide (6.2 g, 30 mmol), and 4-pyrrolidinopyridine (0.48 g, 3 mmol) in dichloromethane (100 mL) was stirred at room temperature for 24 h. The N,N-dicyclohexyl urea was filtered and the filtrate was sequentially washed with water (150 mL), 5% acetic acid solution (150 mL), and water (150 mL), and dried over $MgSO_4$. After evaporation of the solvent, the residue was subjected to column chromatography on silica gel with DCM as eluting solvent to yield white powder (70%). ^{1}H NMR (600 MHz, d_6-DMSO) δ (ppm): 8.10 (m, 4H, ArH), 7.83 (d, 1H, ArH), 7.65 (m, 1H, ArH), 7.50 (d, 1H, ArH), 7.13 (m, 4H, ArH), 6.27, 6.07, 5.88 (3m, 3H, CH_2═CH), 4.38, 4.20 (2t, 4H, −CH_2−O), 4.11 (t, 4H, −CH_2−O), 1.74, 1.46 (2m, 8H, −CH_2−), 0.96 (t, 6H, −CH_3). ^{13}C NMR (150 MHz, d_6-DMSO) δ (ppm): 14.2, 19.2, 31.1, 62.4, 63.6, 68.2, 68.3, 115.2, 115.3, 121.3, 121.5, 124.3, 124.5, 126.0, 128.4, 128.6, 131.9, 132.3, 132.6, 132.7, 148.1, 148.3, 163.7, 163.9, 164.8 and 165.8. IR (KBr, cm^{-1}): 3078 (−C═C−H, s), 2956, 2936, 2870 (C−H, s), 1731 (C═O, s), 1609, 1582, 1512 (Benz. ring, s), 1470 (C−H, δ), 1302, 1250, 1200 1166 (C−O−C, s). EA: C 68.0 (calcd 67.5), H 5.9 (calcd 5.9).

2.4. 3″-Acryloyloxypropyl 2,5-di(4′-butyloxybenzoyloxy)benzoate (3-ADBB)

3-ADBB was similarly prepared as mentioned for the 2-ADBB synthesis. The synthetic details and analytic results of the intermediates A_3 and B_3 are given in the Supporting information. ^{1}H NMR (300 MHz, d_6-DMSO) δ (ppm): 8.10 (m, 4H, ArH), 7.85 (d, 1H, ArH), 7.65 (m, 1H, ArH), 7.49 (d, 1H, ArH), 7.12 (m, 4H, ArH), 6.24, 6.10, 5.88 (3m, 3H, CH_2═CH), 4.20 (t, 2H, −CH_2−O), 4.10 (m, 6H, −CH_2−O), 1.75 (m, 6H, −CH_2−), 1.47 (m, 4H, −CH_2−), 0.95 (t, 6H, −CH_3). ^{13}C NMR (75 MHz, d_6-DMSO) δ (ppm): 14.2, 19.2, 27.8, 31.1, 61.5, 62.2, 68.3, 115.3, 120.9, 121.2, 124.8, 125.0, 126.1, 128.5, 128.7, 132.0, 132.7, 148.1, 148.7, 163.8, 164.2, 164.8 and 165.8. IR (KBr, cm^{-1}): 3077 (−C═C−H, s), 2958, 2934, 2869 (C−H, s), 1731 (C═O, s), 1634 (C═C, s), 1609, 1582, 1512 (Benz. ring, s), 1475, 1392 (C−H, δ), 1251, 1182, 1166, 1075 (C−O−C, s). EA : C 67.9 (calcd 68.0), H 6.1 (calcd 6.1).

Please cite this article in press as: Wei R, et al., Effect of molecular parameters on thermomechanical behavior of side-on nematic liquid crystal elastomers, Polymer (2013), http://dx.doi.org/10.1016/j.polymer.2013.07.057

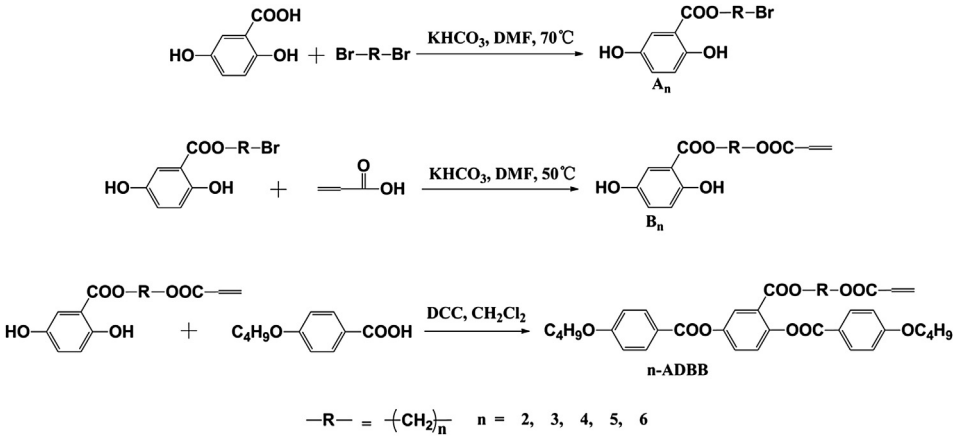

Scheme 1. Synthetic route of the monomers.

2.5. 4″-Acryloyloxybutyl 2,5-di(4′-butyloxybenzoyloxy)benzoate (4-ADBB)

4-ADBB was similarly prepared as mentioned for the 2-ADBB synthesis. The synthetic details and analytic results for the intermediates A_4 and B_4 are given in the Supporting information. ^{1}H NMR (300 MHz, d_6-DMSO) δ (ppm): 8.09 (m, 4H, ArH), 7.84 (d, 1H, ArH), 7.66 (m, 1H, ArH), 7.49 (d, 1H, ArH), 7.12 (m, 4H, ArH), 6.25, 6.13, 5.91 (3m, 3H, CH_2═CH), 4.11 (m, 6H, −CH_2−O), 3.95 (t, 2H, −CH_2−O), 1.72 (m, 4H, −CH_2−), 1.48 (m, 8H, −CH_2−), 0.95 (t, 6H, CH_3). ^{13}C NMR (75 MHz, d_6-DMSO) δ (ppm): 15.3, 20.3, 26.2, 32.2, 65.2, 66.5, 69.4, 116.4, 122.3, 126.1, 126.8, 129.5, 130.0, 132.9, 133.9, 148.8, 149.4, 164.9, 165.2, 165.9 and 166.4. IR (KBr, cm^{-1}): 3075 (−C═C−H, s), 2958, 2934, 2872 (C−H, s), 1732 (C═O, s), 1634 (C═C, s), 1608, 1581, 1512 (Benz. ring, s), 1475, 1389 (C−H, δ), 1252, 1182, 1166, 1073 (C−O−C, s). EA: C 68.2 (calcd 68.3), H 6.3 (calcd 6.3).

2.6. 5″-Acryloyloxypentyl 2,5-di(4′-butyloxybenzoyloxy)benzoate (5-ADBB)

5-ADBB was similarly prepared as mentioned for the 2-ADBB synthesis. The synthetic details and analytic results for the intermediates A_5 and B_5 are given in the Supporting information. ^{1}H NMR (600 MHz, d_6-DMSO) δ (ppm): 8.09 (m, 4H, ArH), 7.83 (d, 1H, ArH), 7.66 (m, 1H, ArH), 7.47 (d, 1H, ArH), 7.13 (m, 4H, ArH), 6.29, 6.13, 5.89 (3m, 3H, CH_2═CH), 4.11 (m, 6H, −CH_2−O), 3.98 (t, 2H, −CH_2−O), 1.74 (m, 4H, −CH_2−), 1.45 (m, 8H, −CH_2−), 1.22 (m, 2H, −CH_2−), 0.96 (t, 6H, −CH_3). ^{13}C NMR (150 MHz, d_6-DMSO) δ (ppm): 14.2, 19.2, 22.3, 28.0, 28.2, 31.1, 64.3, 65.6, 68.3, 68.4, 115.2, 120.9, 121.1, 125.1, 126.1, 128.8, 129.0, 132.5, 132.7, 147.9, 148.6, 163.8, 164.1, 164.6 and 166.0. IR (KBr, cm^{-1}): 3063 (−C═C−H, s), 2958, 2934, 2872 (C−H, s), 1727, 1704 (C═O, s), 1634 (C═C, s), 1604, 1578, 1511 (Benz. ring, s), 1488, 1389 (C−H, δ), 1252, 1163, 1065 (C−O−C, s). EA: C 68.7 (calcd 68.7), H 6.5 (calcd 6.5).

2.7. 6″-Acryloyloxyhexyl 2,5-di(4′-butyloxybenzoyloxy)benzoate (6-ADBB)

6-ADBB was similarly prepared as mentioned for the 2-ADBB synthesis. The synthetic details and analytic results for the intermediates A_6 and B_6 are given in the Supporting information. ^{1}H NMR (300 MHz, $CDCl_3$) δ (ppm): 8.15 (m, 4H, ArH), 7.88 (d, 1H, ArH), 7.46 (m, 1H, ArH), 7.26 (d, 1H, ArH), 6.98 (m, 4H, ArH), 6.35, 6.13, 5.80 (3m, 3H, CH_2═CH), 4.09 (m, 8H, −CH_2−O), 1.81 (m, 4H, −CH_2−), 1.55 (m, 8H, −CH_2−), 1.27 (m, 4H, −CH_2−), 0.99 (t, 6H, −CH_3). ^{13}C NMR (75 MHz, $CDCl_3$) δ (ppm): 13.9, 19.3, 25.6, 28.4, 28.5, 31.2, 53.5, 64.5, 65.5, 68.1, 114.4, 114.5, 121.1, 121.5, 125.1, 127.2, 128.7, 130.5, 132.4, 132.5, 148.1, 148.4, 163.7, 164.2, 164.7 and 166.3. IR (KBr, cm^{-1}): 3063 (−C═C−H, s), 2957, 2935, 2871 (C−H, s), 1732 (C═O, s), 1634 (C═C, s), 1608, 1581, 1513, 1480 (Benz. ring, s), 1492, 1389 (C−H, δ), 1251, 1166, 1073 (C−O−C, s). EA: C 69.0 (calcd 69.1), H 6.7 (calcd 6.7).

2.8. Polymerization of the monomers in solution

To test the polymerization ability, the monomers were also polymerized in solutions. Description of the radical polymerization

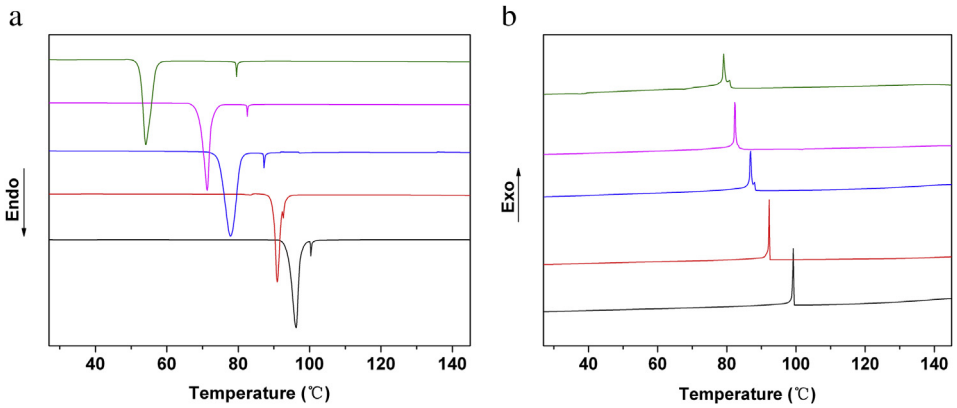

Fig. 1. DSC curves of the monomers: a. DSC curves of the monomers in the first heating scan, from bottom to top: 2-ADBB, 3-ADBB, 4-ADBB, 5-ADBB and 6-ADBB; b. DSC curves of the monomers in the first cooling scan, from bottom to top: 2-ADBB, 3-ADBB, 4-ADBB, 5-ADBB and 6-ADBB.

Please cite this article in press as: Wei R, et al., Effect of molecular parameters on thermomechanical behavior of side-on nematic liquid crystal elastomers, Polymer (2013), http://dx.doi.org/10.1016/j.polymer.2013.07.057

Table 1
The T_{NI} of the monomers obtained from DSC and POM observation; T_{NI} of the LCE micropillars estimated from POM observation, where the crosslinking agent content was 20 mol%.

	T_{NI} °C (DSC) monomer	T_{NI} °C (POM) monomer	T_{NI} °C (POM) LCE pillars
2-ADBB	100	104	110
3-ADBB	92	95	115
4-ADBB	87	88	125
5-ADBB	82	85	116
6-ADBB	79	81	115

in solution of the monomers and characterization of the corresponding side-on polymers are given in the Supporting information.

2.9. Preparation of PDMS molds

Photoresist was spin-coated on a piece of pre-cleaned silicon wafers and dried in vacuum. The thickness of the photoresist was set to about 100 μm by controlling the spinning speed. A photomask with $\varphi = 20$ μm hole array was placed in contact with the surface of the photoresist. After illumination with ultraviolet (UV) light through the mask, the photoresist not crosslinked was dissolved and removed by an organic solvent. The master with pillar array of photoresist in bas-relief on the surface was obtained. The poly(dimethylsiloxane) (PDMS) molds were obtained by mixing the elastomer base and curing agent (Dow Corning, Sylgard 184) in a proper ratio (10:1, *w*/*w*). The prepolymer was poured and casted on the master surface and then cured in a 40 °C oven for 4 h. After curing, the PDMS molds were separated from the master and used afterwards without any more treatment.

2.10. Fabrication of pillars

Monomers and crosslinking agent 1,6-hexanediol diacrylate in different ratios were mixed with 2% photoinitiator 2-benzyl-2-(dimethylamino)-4′-morpholinobutyrophenone, using dichloromethane as a solvent. According to the literature [13,14], a small amount of the mixture was heated to the isotropic phase (100 °C) on a microscope slide positioned atop a rare earth permanent magnet (1 T NdFeB rare earth magnet). The PDMS mold was then gently pressed down on the melted sample, which filled the inner structure of the mold. The temperature was then slowly decreased (1 °C/min) down to 60 °C, at which the sample is in its nematic phase. For 6-ADBB, the temperature was decreased down to 45 °C due to the fact that the T_{NI} is lower than 60 °C. Then the sample was irradiated with the UV light from a high pressure mercury lamp (1000 W, equipped with quartz jacket condenser cooled with running water) for 1 h for the polymerization and crosslinking. The distance between the sample and lamp was about 25 cm. The whole setup was shielded by quartz cover through which argon flow could get through to ensure an inert atmosphere above the sample. The argon gas protection was kept until the polymerization and crosslinking were completed. After cooling to room temperature, the PDMS mold was peeled off, leaving a thin glassy polymer film covered by a regular array of pillars. Separate pillars were obtained by carefully cutting them off from the substrate with a razor blade and suspending them in silicon oil.

3. Results and discussion

3.1. Synthesis and characterization

The synthetic route used to prepare the monomers (*n*-ADBB) is shown in Scheme 1, which includes three reaction steps. Firstly, a nucleophilic substitution reaction between the carboxylate group of 2,5-dihydroxybenzoic acid and one of the bromine in α,ω-dibromoalkanes was carried out under mild conditions. Then, the second bromine was substituted with the reactive acrylate group using the same procedure. Finally, the monomers were obtained by esterification of the previous intermediates with 4-n-butyloxybenzoic acid under standard conditions (activated by dicyclohexylcarbodiimide and catalyzed by 4-pyrrolidinopyridine). This newly developed procedure is simple and straightforward compared with the previously reported scheme [11,41]. It allowed us to efficiently synthesize monomers *n*-ADBB with different spacer lengths ($n = 2, 3, 4, 5, 6$). The analytical results, obtained from ^{1}H NMR, ^{13}C NMR, and FT-IR, are given in the Experimental section and ^{1}H NMR spectra with resonance signal assignments are given in the Supporting information. The results confirmed that the series of the nematic side-on acrylate monomers were successfully synthesized.

The mesomorphic properties of the monomers were characterized by DSC and POM. Fig. 1 shows the DSC curves of the monomers on the first heating (Fig. 1a) and first cooling (Fig. 1b)

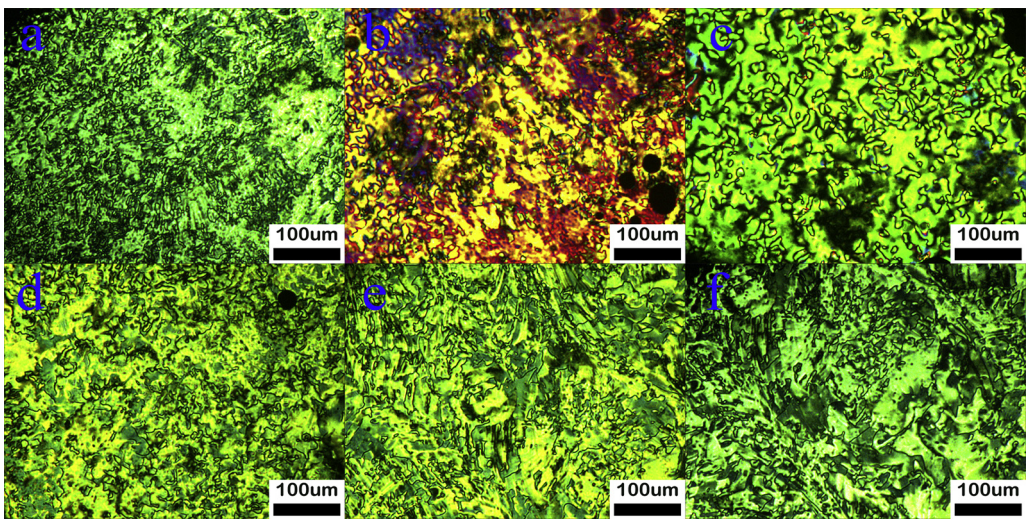

Fig. 2. POM images of the monomers. a. 2-ADBB at 103 °C; b. 3-ADBB at 94 °C; c. 4-ADBB at 87 °C; d. 5-ADBB at 84 °C; e. 6-ADBB at 65 °C; f. 6-ADBB at 80 °C.

Please cite this article in press as: Wei R, et al., Effect of molecular parameters on thermomechanical behavior of side-on nematic liquid crystal elastomers, Polymer (2013), http://dx.doi.org/10.1016/j.polymer.2013.07.057

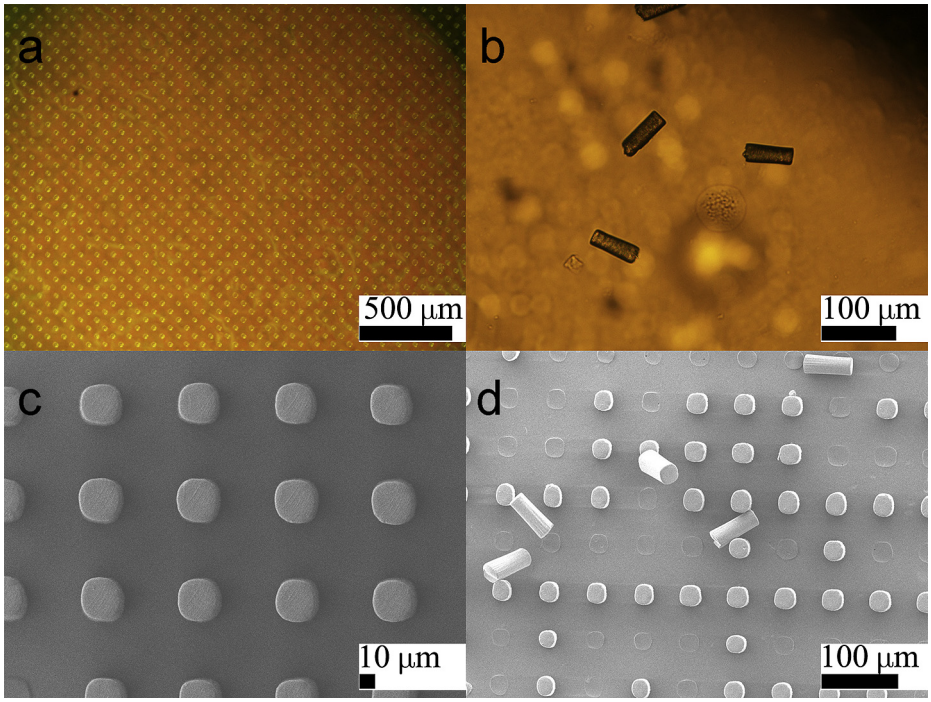

Fig. 3. Optical micrographs and SEM images of the LCE micropillars: a. optical microscopic graphs of the array of the LCE pillars; b. separate LCE pillars suspended in silicon oil; c. and d. SEM images of LCE pillars. The LCE pillars were obtained from 4-ADBB with the 20 mol% crosslinking agent.

scans. 2-ADBB melts at 96 °C (peak value) and shows a small endothermic transition at 100 °C (peak value), which corresponds to the clearing point (T_{NI}) of the monomer on heating. On the cooling scan, an exothermic transition around 100 °C (peak value) is observed for 2-ADBB, while no crystallization peak can be detected. The other monomers show lower melting and clearing points as the spacer length increases (Fig. 1 and Table 1). POM observations confirm that all the monomers enter the nematic phase after melting. Fig. 2 shows some representative images of the textures observed by POM.

In order to compare with the properties of the LCEs, the monomers were also polymerized by radical polymerization in solution. The characterization of the corresponding side-on liquid crystalline polymers gives further information on the physical properties in particular their mesomorphic properties. The obtained polymers have average molecular weights (M_n) around 10,000 and polydispersities (PDI) below 2.5 (Table S1, in the Supporting information). The phase transition temperatures obtained by both DSC and POM observation are also given there. All the polymers exhibit a nematic mesophase in proper temperature ranges. The nematic-isotropic transition temperatures (T_{NI}) of the polymers decrease with the spacer length increase.

3.2. Fabrication of micropillar arrays and separate micropillars

Using the nematic acrylate monomers synthesized above, LCEs were prepared under the form of thin films covered with micropillars. The method was described in the Experimental section and also in the previous reports in detail [13,14]. In the process, monomers and crosslinking agent 1,6-hexanediol diacrylate in different ratios were mixed with 2% (mol%) of the photoinitiator, 2-benzyl-2-(dimethylamino)-4′-morpholinobutyrophenone. After heated the mixture to the isotropic phase, a piece of the PDMS mold was gently pressed down on the melted sample, which filled the inner column-shaped structures of the mold. When the sample was cooled down to enter the nematic phase with the magnetic field alignment, it was irradiated by the UV light with the argon gas protection for the polymerization and crosslinking. A thin glassy polymer film covered by a regular array of pillars was obtained after cooling to room temperature and peeling off the PDMS mold.

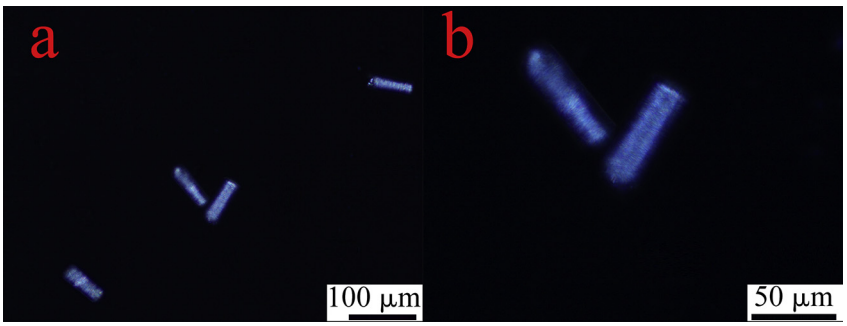

Fig. 4. POM images of micropillars obtained from 4-ADBB with the 5 mol% crosslinking agent, observed at room temperature.

Please cite this article in press as: Wei R, et al., Effect of molecular parameters on thermomechanical behavior of side-on nematic liquid crystal elastomers, Polymer (2013), http://dx.doi.org/10.1016/j.polymer.2013.07.057

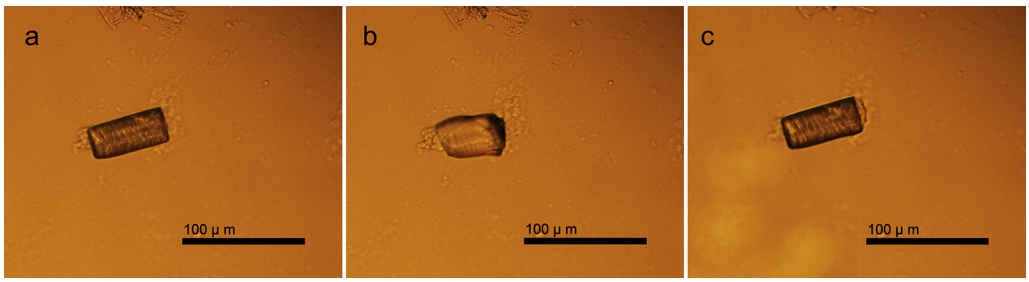

Fig. 5. The optical micrographs of a single LCE pillar at different temperatures: a. room temperature; b. 130 °C; c. room temperature again. The LCE pillar was obtained from 4-ADBB with 15 mol% crosslinking agent.

Separate micropillars were obtained from the pillar array by carefully cutting them off from the substrate with a razor blade.

Fig. 3 shows the optical microscope and SEM images of the micropillar array and separate pillars. In Fig. 3a, the optical microscope image shows regular alignment of the micropillars in the array on a large scale. It indicates that micro-structures with uniform sizes can be obtained with a high efficiency by this method. Fig. 3b shows the optical microscope image of the separate pillars suspended in silicon oil. The average length of the micropillars was measured to be around 62 μm Fig. 3c and 3d shows the SEM images of the pillars for different amplification scales. The pillar sizes were also measured from the SEM images by carefully cutting off the pillars before the sputtering treatment. The lengths of the micropillars were estimated to be about 60 μm. For all five monomers prepared in this work, the well-defined pillar-like microstructures were obtained and used for the following investigations. Fig. 4 gives some typical POM images of the separate micropillars placed between the crossed polarizers and observed at the room temperature. The bright images due to the birefringence evidence the mesogenic alignment in the micropillars. Similar optical anisotropy is observed for the micropillars obtained from the other monomers with different spacer lengths.

3.3. *Effect of the crosslinking density*

The effect of the degree of crosslinking on the thermomechanical behavior of the LCEs was studied by using the micropillars. The result obtained for 4-ADBB is presented below to elucidate the effect. In the experiment, 4-ADBB and 2 mol% photoinitiator were mixed with 5, 10, 15, 20 and 25 mol% of crosslinking agent 1,6-hexanediol diacrylate, respectively. The regular arrays of LCE micropillars on glass substrates and separate micropillars were obtained from these samples by the method mentioned above. The shape changes of these individual micropillars, suspended in silicon oil to prevent them from sticking on the microscope glass slides, were studied as a function of the temperature by POM equipped with the hot stage.

Fig. 5 shows typical optical micrographs of a single LCE micropillar obtained from 4-ADBB with 15 mol% of the crosslinking agent at room temperature (Fig. 5a and c) and 130 °C (Fig. 5b). By heating to a temperature above the nematic-to-isotropic phase transition temperature of the LCE, a significant contraction of the micropillar in the longitudinal direction is observed. While cooling back to room temperature, the micropillar recovers its original shape. As the micropillars prepared by this method are uniform, the thermomechanical deformation in the same scale is also observed for other pillars in the array. It can be estimated from the micrographs that the micropillar contracts up to 77% of the original length in the longitudinal direction.

To better understand the thermomechanical properties of the LCEs, the contraction and relaxation were measured as a function of the temperature with a slow temperature variation (with the heating and cooling rates ±1 °C per minute) from 100 °C to 130 °C and back. Fig. 6 shows the deformation of the micropillars with the temperature, where the pillars were made from 4-ADBB and different contents of the crosslinking agent. The deformation in the figure is given as the length ratio between the contracted pillar and the original one, and the content of crosslinking agent is presented by the molar percentage. All the LCE micropillars show significant contraction except the one with 25% crosslinking agent. It can be attributed to the high crosslinking density in the system. With high concentration of the crosslinking agent, too many crosslinking junctions are introduced, which causes the sample to change from an elastomer to a thermoset. It is interesting to note that a sudden change occurs when the crosslinking agent increases from 20% to 25%. This process can be rationalized by considering a percolation change with the crosslinking density. Among the LCE micropillars showing the thermomechanical responses, the one with 5% crosslinking agent exhibits the largest contraction, reflecting the fact that it is a softer elastomer. The measured contractions are 39%, 30%, 27%, 24% and 0% (the contraction is defined as $(L_0 - L_T)/L_0$) for micropillars with crosslinking agent content of 5%, 10%, 15%, 20% and 25% respectively. The temperatures for the LCE micropillars to reach the maximum contraction decrease with the increasing crosslinking agent contents in a few-degree scale. The LCE micropillar with 5% crosslinking agent shows the highest transition temperature among them. This observation can be attributed to the flexible and non-mesogenic nature of the crosslinking agent, where the increase in its content will cause the decrease of orientational order and T_{NI}.

Above result indicates that 5% of the crosslinking agent seems to be sufficient to transform a visco-elastic polymer melt into an

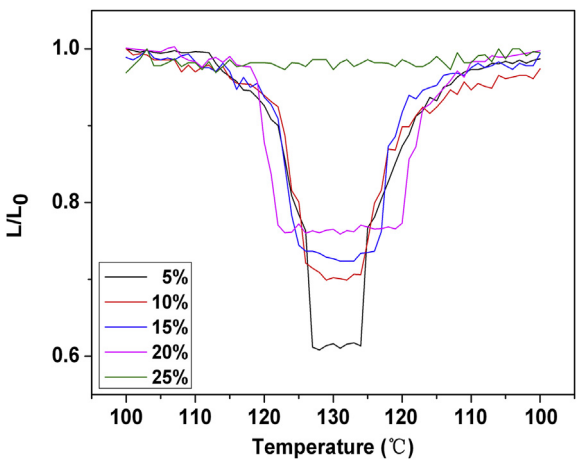

Fig. 6. The length change of the LCE pillars with different contents of crosslinking agent versus the changing temperature. The LCE pillars were obtained from 4-ADBB.

Please cite this article in press as: Wei R, et al., Effect of molecular parameters on thermomechanical behavior of side-on nematic liquid crystal elastomers, Polymer (2013), http://dx.doi.org/10.1016/j.polymer.2013.07.057

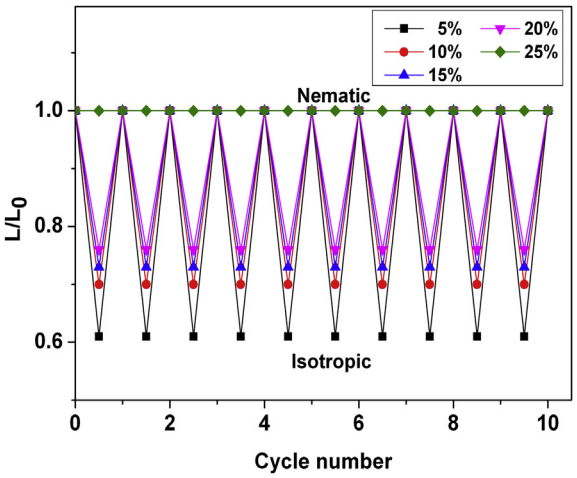

Fig. 7. The reversible switch between contraction and extension of the LCE pillars obtained from 4-ADBB.

elastomer. To further confirm this point, the thermomechanical deformation behavior was investigated through repeated contraction–extension variations by cycling up to ten times. The good reversibility and robustness shown in Fig. 7 verify the elasticity of the materials. This result not only shows the potential applicability of this kind of LCE materials but also indicates that the addition of the 5% crosslinking agent is enough to introduce the crosslinking density above the threshold value.

3.4. Effect of the spacer length

The result obtained from 4-ADBB as the representative shows that LCE microstructure with reversible thermomechanical deformation can be obtained by introducing a proper amount of crosslinking points. By similar method, LCE micropillars were prepared from the other synthesized acrylate monomers to study the effect of the spacer length on the properties. In all experiments reported below, the concentration of the crosslinking agent was fixed to be 20 mol%. The results observed on samples with concentrations of the crosslinking agent of 5, 10, 15 mol% are similar.

Fig. 8 shows the contraction and expansion of the micropillars made from this series of monomers with the temperature variation. The deformation in the figure is given as the length ratio of the contracted pillar to the original one. The micropillars made from 2-ADBB exhibit the largest contraction of about 31% and the contraction becomes smaller as the spacer length of the monomer increases (Fig. 8a). As the spacer lengths increase, the contraction gradually becomes smaller when the spacer length increases from 2-ADBB to 6-ADBB. The result shows that the coupling between the mesogenic units and backbone is important to force the polymer chain to take an anisotropic conformation. As the short spacer in 2-ADBB forces the backbone to take a more anisotropic shape, which acts more or less like a main-chain liquid crystal polymer, a larger contraction will occur at the nematic to isotropic phase transition. When the spacer length becomes longer, the coupling between the mesogens and backbone through the spacers becomes weaker. The monomer possessing a long spacer, such as 6-ADBB, could behave more similar to an end-on side-chain liquid crystal polymer. For all samples, when the temperature gradually decreases, the micropillars show the reversible expansion as shown in Fig. 8b.

Another remarkable point that can be seen from Fig. 8 is that the transition temperature of the LCEs is also closely related to the spacer length. However, the result shows a somewhat irregular variation of the transition temperatures with the spacer length increase. The micropillars obtained from 4-ADBB show the highest transition temperature compared with others. To understand this phenomenon, the T_{NI} values of LCE micropillars were obtained from the POM observation and compared with the temperatures for the micropillars to reach the maximum contraction. The T_{NI} of LCE micropillars obtained from the POM observation is given in Table 1 together with the transition temperatures of the corresponding monomers. The T_{NI} values are 110, 115, 125, 116, and 115 °C for LCE micropillars obtained from 2-ADBB, 3-ADBB, 4-ADBB, 5-ADBB, and 6-ADBB. Compared with the thermomechanical deformation behavior shown in Fig. 8a, it can be seen that for the LCE micropillars obtained from 2-ADBB, 3-ADBB, and 5-ADBB, the temperature to reach the maximum contraction is about the 5–10 °C lower compared to the corresponding T_{NI} values. On the contrary, the temperatures for LCE micropillars obtained from 4-ADBB and 6-ADBB to reach the maximum contraction are almost the same as the corresponding T_{NI}.

The observations indicate that the relationship between the thermomechanical transition temperature and spacer length can be attributed to the two contradictory factors that influence the transition temperature. As indicated by the result given in Fig. 1 and Table 1, the clearing temperatures of the monomers decrease with the increasing spacer length. Similar relationship can also be seen for corresponding linear polymers obtained from the monomers through the radical polymerization (Table S1, in the Supporting information). Therefore, the transition temperature of LCEs should show a similar tendency with the spacer length variation.

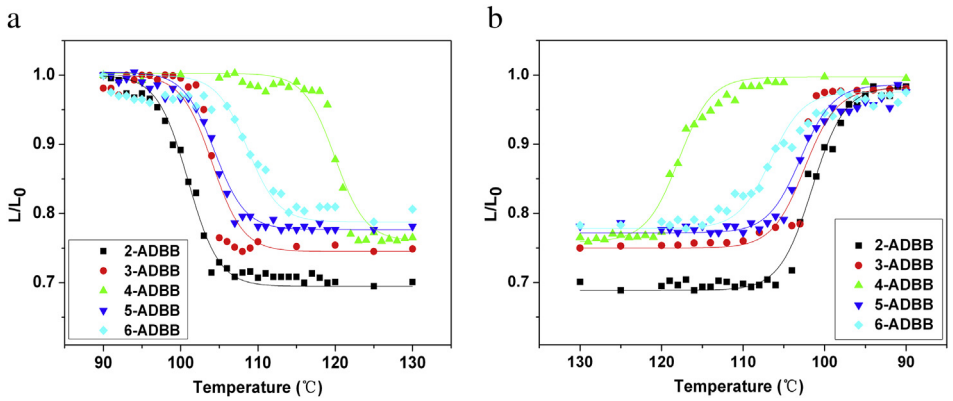

Fig. 8. The length change of the LCE pillars made from the monomers: a, contraction, b, expansion. The content of the crosslinking agent was 20 mol%.

Please cite this article in press as: Wei R, et al., Effect of molecular parameters on thermomechanical behavior of side-on nematic liquid crystal elastomers, Polymer (2013), http://dx.doi.org/10.1016/j.polymer.2013.07.057

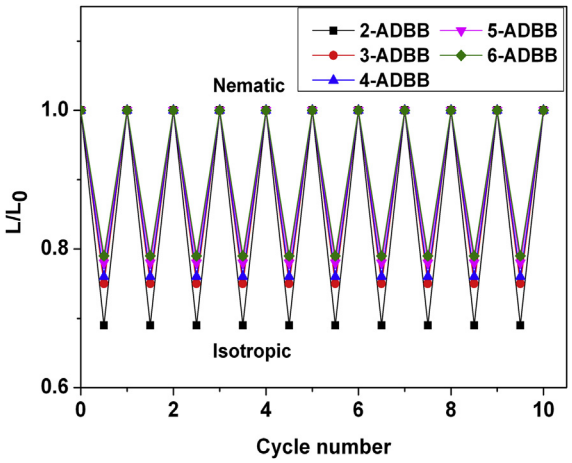

Fig. 9. The reversible switch between contraction and extension of the LCE pillars obtained from the monomers. The content of crosslinking agent was 20 mol%.

This tendency can be seen for LCEs obtained from 4-ADBB, 5-ADBB, and 6-ADBB. On the other hand, LCE with the short spacer has the strong correlation between the mesogens and backbone. As a result, the polymeric chains between the crosslinks will be distorted more significantly with respect to the equilibrium conformation. This departure from the equilibrium can be treated as an internal tension, which will trigger the relaxation to occur at a lower temperature to maximize the entropy. This internal tension is the cause for LCEs obtained from 2-ADBB, 3-ADBB and 5-ADBB to reach the maximum contraction at the temperatures about the 5–10 °C below the corresponding T_{NI} values. As another evidence of this internal tension, it can be seen from the data in Table 1 that the LCE pillars obtained from 2-ADBB show the smallest increase in T_{NI} after the polymerization and crosslinking. The LCE pillars obtained from 4-ADBB show the largest increase in T_{NI} after the polymerization and crosslinking. Therefore, the T_{NI} values for LCEs obtained from 2-ADBB and 3-ADBB are actually lower than that of LCE obtained from 4-ADBB. This understanding can be used to explain why the micropillars obtained from 2-ADBB and 3-ADBB show the lower thermomechanical transition temperatures compared with that of 4-ADBB. The lower thermomechanical transition temperatures of LCEs obtained from 5-ADBB and 6-ADBB can be attributed to the lower T_{NI} for the monomers and polymers. However, due to the internal tension, T_{NI} and the thermomechanical transition temperature of LCE obtained from 5-ADBB appear to be lower than that it should be.

Similar to the result given in Fig. 7, a good reversibility and robustness can also be observed for the LCEs with the different spacer lengths. Fig. 9 shows the repeated contraction–extension variations by cycling up to ten times, which verifies the good elasticity of the materials. Above result indicates that for the systems with the proper amount of the crosslinking agent, the spacer length variation from 2 to 6 methylenes shows no influence on transformation from visco-elastic to elastic after the crosslinking.

4. Conclusions

In order to investigate the structure–property relationship, we synthesized a series of nematic side-on liquid crystal acrylate monomers (*n*-ADBB) by a modified synthetic strategy. The monomers were characterized by ^{1}H NMR, ^{13}C NMR, FT-IR, POM and DSC. LCE micropillars were made from these newly synthesized monomers by the soft lithography and photopolymerization/photocrosslinking.

The crosslinking density of the LCEs showed a significant influence on the thermomechanical properties of LCEs. If the density of the crosslinking points was too high, such as the system with 25% crosslinking agent, no thermal-induced contraction could be observed. The observed contractions changed from 39%, 30%, 27% to 24% for the micropillars with the crosslinking agent content of 5%, 10%, 15% and 20%, respectively. The 5 mol% amount of the crosslinking agent was sufficient to transform a visco-elastic polymer melt into an elastomer.

The spacer length of the LCEs was another important factor to influence the thermomechanical properties of LCEs. For LCEs with the short spacer, the coupling between the mesogens and polymer main-chain was strong, which induced a more anisotropic chain conformation. The micropillars made from 2-ADBB showed the largest contraction of about 31% and the contraction decreased as the spacer length in the monomers became longer. For the systems with a proper amount of the crosslinking agent, the spacer length variation from 2 to 6 methylenes showed no influence on the elasticity.

Acknowledgment

The financial support from the NSFC under Projects 91027024, 51233002 and 51061130556, from the French ANR under Project ANR-10-INTB-0904 and a PICS-CNRS project is gratefully acknowledged.

Appendix A. Supplementary data

Supplementary data related to this article can be found at http://dx.doi.org/10.1016/j.polymer.2013.07.057.

References

[1] Warner M, Terentjev EM. Liquid crystal elastomers. Oxford, UK: Oxford University Press; 2003.
[2] Finkelmann H, Kim ST, Munoz A, Palffy-Muhoray P, Taheri B. Adv Mater 2001;13(14):1069–72.
[3] Ikeda T, Nakano M, Yu YL, Tsutsumi O, Kanazawa A. Adv Mater 2003;15(3):201–5.
[4] Ji Y, Huang YY, Rungsawang R, Terentjev EM. Adv Mater 2010;22(31):3436–40.
[5] Li MH, Keller P, Li B, Wang XG, Brunet M. Adv Mater 2003;15(7–8):569–72.
[6] Ohm C, Serra C, Zentel R. Adv Mater 2009;21(47):4859–62.
[7] van Oosten CL, Bastiaansen Cees WM, Broer DJ. Nat Mater 2009;8(8):677–82.
[8] Lehmann W, Skupin H, Tolksdorf C, Gebhard E, Zentel R, Krüger P, et al. Nature 2001;410(6827):447–50.
[9] Yoshino T, Kondo M, Mamiya JI, Kinoshita M, Yu YL, Ikeda T. Adv Mater 2010;22(12):1361–3.
[10] Yamada M, Kondo M, Mamiya JI, Yu YL, Kinoshita M, Barrett CJ, et al. Angew Chem Int Ed 2008;47(27):4986–8.
[11] Thomsen DL, Keller P, Naciri J, Pink R, Jeon H, Shenoy D, et al. Macromolecules 2001;34(17):5868–75.
[12] Cotton JP, Hardouin F. Prog Polym Sci 1997;22(4):795–828.
[13] Buguin A, Li MH, Silberzan P, Ladoux B, Keller P. J Am Chem Soc 2006;128(4):1088–9.
[14] Yang H, Buguin A, Taulemesse JM, Kaneko K, Méry S, Bergeret A, et al. J Am Chem Soc 2009;131(41):15000–4.
[15] Finkelmann H, Nishikawa E, Pereira GG, Warner M. Phys Rev Lett 2001;87(1):015501, 4 pages.
[16] Yu YL, Nakano M, Ikeda T. Nature 2003;425(6954):145.
[17] Courty S, Mine J, Tajbakhsh AR, Terentjev EM. Europhys Lett 2003;64(5):654–60.
[18] Huang C, Zhang QM, Jákli A. Adv Funct Mater 2003;13(7):525–9.
[19] Urayama K, Honda S, Takigawa T. Macromolecules 2005;38(9):3574–6.
[20] Ohm C, Brehmer M, Zentel R. Adv Polym Sci 2012;250:49–94.
[21] Chen ML, Xing X, Liu Z, Zhu YT, Liu H, Yu YL, et al. Appl Phys A-Mater 2010;100(1):39–43.
[22] Chen ML, Huang HT, Zhu YT, Liu Z, Xing X, Cheng FT, et al. Appl Phys A-Mater 2011;102(3):667–72.
[23] Fleischmann1 EK, Liang HL, Kapernaum N, Giesselmann F, Lagerwall J, Zentel R. Nat Commun 2012;3:1178–85.
[24] Serak S, Tabiryan N, Vergara R, White TJ, Vaia RA, Bunning TJ. Soft Matter 2010;6(4):779–83.
[25] Ogawa H, Stibal-Fischer E, Finkelmann H. Macromol Chem Phys 2004;205(5):593–9.

[26] Beyer P, Braun L, Zentel R. Macromol Chem Phys 2007;208(22):2439–48.
[27] Bispo M, Guillon D, Donnio B, Finkelmann H. Macromolecules 2008;41(9):3098–108.
[28] Finkelmann H, Rehage G. Adv Polym Sci 1984;60/61:99–172.
[29] Gray GW, Hill JS, Lacey D. Mol Cryst Liq Cryst 1991;197(1):43–55.
[30] Mu J, Okamoto H, Yanai T, Takenaka S, Feng XS. Colloid Surf A 2001;181(1–3):303–13.
[31] Lecommandoux S, Achard MF, Hardouin F. Liq Cryst 1998;25(1):85–94.
[32] Achard MF, Lecommandoux S, Hardouin F. Liq Cryst 1995;19(5):581–7.
[33] (a) Ober CK, Jin J, Zhou QF, Lenz RW. Adv Polym Sci 1984;59:103–46;
(b) Chen S, Luo H, Xie HL, Zhang HL. Polymer 2013;54(7):1794–802.
[34] Chen XF, Shen ZH, Wan XH, Fan XH, Chen EQ, Ma YG, et al. Chem Soc Rev 2010;39(8):3071–101.
[35] Yu YL, Nakano M, Shishido A, Shiono T, Ikeda T. Chem Mater 2004;16(9):1637–43.
[36] Küpfer J, Finkelmann H. Macromol Rapid Commun 1991;12(12):717–26.
[37] Ohm C, Brehmer M, Zentel R. Adv Mater 2010;22(31):3366–87.
[38] Ohm C, Kapernaum N, Nonnenmacher D, Giesselmann F, Serra C, Zentel R. J Am Chem Soc 2011;133(14):5305–11.
[39] Ohm C, Haberkorn N, Theato P, Zentel R. Small 2011;7(2):194–8.
[40] Wei RB, He YN, Wang XG, Keller P. Macromol Rapid Commun 2013;34(4):330–4.
[41] Keller P, Thomsen DL, Li MH. Macromolecules 2002;35(2):581–4.

Please cite this article in press as: Wei R, et al., Effect of molecular parameters on thermomechanical behavior of side-on nematic liquid crystal elastomers, Polymer (2013), http://dx.doi.org/10.1016/j.polymer.2013.07.057